Comparison of Si and GaN Power Devices Used in PV Module Integrated Converters

M. Acanski, J. Popovic-Gerber, and J. A. Ferreira
Electrical Sustainable Energy, Electrical Power Procesing
Delft University of Technology
Delft, The Netherlands
E-mail: m.acanski@tudelft.nl

Abstract— **Using the newly developed enhancement-mode Galium-Nitride-on-Silicon (eGaN) devices with high conductivity and very fast switching speed a breakthrough in switching performance can be achieved. Multi-megahertz switching frequency capability will significantly reduce the size of passive components, adding the cost benefits and increasing the integration level and power density. As to date, the use of GaN devices in power converters is still in its infancy, but its widespread application is a near reality. PV converter industry is one of the areas which would greatly benefit from the new GaN technology. The most important requirements for a PV converter, efficiency and cost effectiveness, can both be addressed with improved switching devices. This paper presents a performance comparison of a PV module integrated DC-DC converter based on commercially available GaN and Si power devices. The presented results show that the first generation of GaN devices outperforms the best in class Si devices. Since GaN is immature technology, further improvements will be seen in the years to come.**

I. INTRODUCTION

Ever since early years of power electronics, the power density of electronic converters has been continuously increased in order to meet strengthen demands for size and cost reduction. To date, the main driving force behind this progress was reduction in size of passive components by increasing the conversion switching frequency. Today, after many years of constant development the current Si technology has approached its limits and slowed down to the point where small improvements have significant development costs. The major barriers to the further increase of switching frequency and power density are losses in active devices and the size of thermal management, caused by physical constraints of the Si technology. An alternative approach to further improve the power density is to use novel integration technologies [1] or improved assembly [2]. However the size of passive components, which is primarily determined by switching frequency, still represents the major limitation toward achieving high power density.

Nowadays, a large effort has been devoted to the development of wide-bandgap power semiconductor devices. Recent breakthroughs in processing Gallium Nitride (GaN) have produced enhancement mode devices with high conductivity and very fast switching speed while still keeping silicon-like cost structure and MOSFET-like behavior [3]. The first generation of commercially available GaN transistors already offers significantly improved figures of merit (FOM) compared to the currently available Si technology which brings a disruptive improvement in switching performance.

Power electronic applications can leverage on the development of GaN technology, but the use of GaN devices in power converters is still in its infancy. However, the first power converter applications of GaN technology are beginning to appear in the recent literature. The performance of GaN devices has already been demonstrated in case of the boost converter [4]-[6] and also using commercially available GaN devices in the dual active bridge converter [7].

PV converter industry is one of the areas which would greatly benefit from the new GaN technology. With improvements in switching performance, the PV converter efficiency can be significantly improved. However, in conventional PV architectures, the overall system yield does not rely on the converter efficiency alone but also depends on environmental conditions. Nowadays, as the PV energy penetrates into the residential grid and urban area, the PV system faces new problems. Suboptimal module orientation, shading, soiling and age related mismatch caused by conventional centralized maximum power point tracking can significantly reduce the system power output.

Recently there is a trend in PV systems toward a more granular processing of the PV array power by means of distributed maximum power point tracking (DMPPT) [8]. This is achieved by connecting a DC-DC converter to each PV module in a PV system and thus performing power processing on a module level, as opposed to centralized power processing in traditional PV system architectures (Fig. 1). In that way the power output of each module is optimized regardless of the performance of other modules connected in the same PV array. The mismatch related losses are effectively eliminated, but to make this approach viable the cost of added converters should be compensated by the cost

978-1-4577-0541-0/11/$26.00 ©2011 IEEE

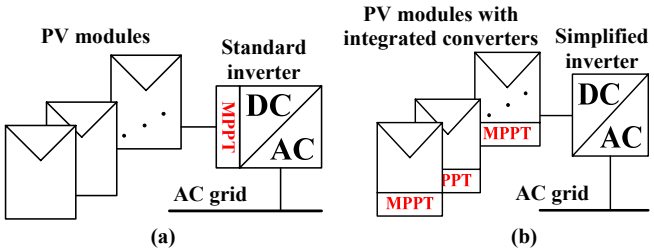

Figure 1. (a) Convential PV system, (b) PV system with DMPPT

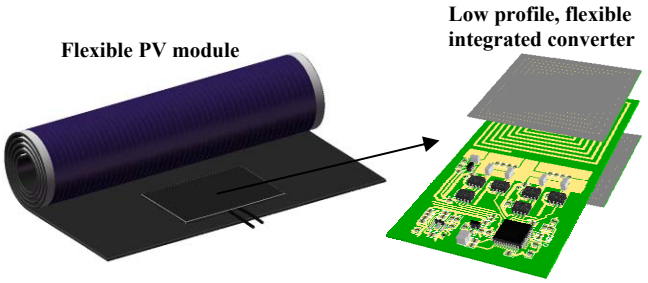

Figure 2. Concept of the PV module integrated converter

of recovered energy. This calls for novel technologies that could reduce the price of power electronics for PV systems.

II. PV Module Integrated Converter Concept

The PV optimization market has evolved rapidly over a short period of time and a number of companies are now offering converters for DMPPT PV systems. For the best system performance, the converter should be optimally designed for the particular PV module that is going to be used. On the other hand, the available solutions are usually designed to be more flexible in terms of electrical specifications in order to meet various voltage and power levels of available PV modules. This imposes additional constraints on the converter design optimization and has a negative effect on the conversion efficiency. Another consideration is the installation cost, since additional cables and connectors together with providing a place for the converter requires additional installation material and labor.

To reduce the cost and to improve the level of integration, it is possible to integrate the converter directly on the back side of the PV module, eliminating additional wires and connections. This also allows for an optimal design of the converter since the electrical specifications of the used PV module are already known. Further improvements in system cost and flexibility can be achieved using recently developed flexible PV modules [9]. A major advantage of flexible PV modules is the potential to lower manufacturing costs through cheap roll-to-roll processing while at the same time offering the same efficiency as the commonly available glass PV modules. Furthermore, such lightweight and flexible solar modules offer additional cost benefits in terms of transportation, installation, structural frames for the modules etc., i.e. they significantly reduce the so-called "balance of system" costs. Taken together, the new flexible PV modules exhibit numerous advantages for applications such as facades, solar farms and BIPV systems.

Fig. 2 illustrates a concept of the DC-DC converter integrated into a flexible PV module. To reduce the cost and improve the level of integration by reducing the number of packaging layers, the back layer of the PV module can be used as a substrate instead of a standard printed circuit board [10]. After the component placement, the converter can be encapsulated for protection using the same back encapsulation material as the PV module. Since the PV module is frameless, suitable supporting structure has to be provided. With a converter placed between the PV module and the supporting surface, flexibility and very low profile become main construction design goals for the module integration. Integration of the converter into the PV module will, on the other hand, impose harsh environmental conditions on the converter operation with elevated temperatures and large temperature swings. PV modules are relatively simple and robust devices and it is a challenge to design a converter that can meet the reliability and lifetime of PV modules. Furthermore, a tight thermal coupling between the converter and the PV module and requirements for low profile and flexible construction introduces interdependence between different areas of the design process. Three main groups of specifications can be identified in the design process of the module integrated converter, electrical, thermal and technological, each with its own trade-offs and sets of boundary conditions.

A. *Electrical requirements*

The main goal of the electrical design is to meet the efficiency requirements and the PV module electrical specifications, while keeping the losses and reached temperatures within the safe area. All this has to be achievable within the available volume. Using a lower switching frequency and more distributed topologies, the requirements for the thermal design can be lowered, at the expense of the required volume and cost, while by increasing the switching frequency the size of passive components can be reduced at the expense of the heat loss density. Therefore, for the selected topology, the switching frequency represents the main trade-off parameter to create balance between the system power density and temperature behavior.

B. *Thermal requirements*

PV modules are relatively inefficient devices with usually more than 80% of the absorbed light energy transformed into heat. Under high irradiation and poor ventilation, the PV module operating temperature can easily reach 70°C or more [11]. With its presence, the integrated converter may block the heat flow from the PV module and add the additional heat through the power losses in its components, creating a hot-spot on the PV module surface. It is therefore the purpose of the converter's thermal management to remove the excess heat without causing negative effects on reliability of the PV module. The reached temperatures can be minimized by reducing the losses through the electrical design and effectively extracted and transferred to the ambient through the thermal design.

C. *Technology requirements*

The main goal of the spatial design is to meet the desired volume and mechanical requirements. This means that, in case of the PV module integration, special technologies are necessary to achieve low profile and flexible design. Low profile design imposes additional burden on the thermal management, since efficient heat spreading has to be implemented in order to extract the heat from active devices and spread it over the large area. Another major barrier to meet the low profile and flexible requirements are magnetic components, although recent achievements show that this can also be addressed by using special core materials [12]. Increasing the switching frequency will certainly benefit the volumetric requirements since the size of magnetic components can be reduced.

Fig. 3 shows the main sets of specifications and interdependence relations in the design of module integrated converter. Both the thermal and spatial designs can benefit from newly developed GaN devices. Faster switching can reduce the required volume for the same amount of allowed losses, or reduce the losses for the case when the original volume is kept. On the other hand, the switching frequency cannot easily rise to very high levels, since the upper limit is constrained by the parasitic components, circuit layout and EMI requirements. Therefore, improvement of switching devices alone is not enough to achieve high power densities; it also has to be followed by novel packaging technologies.

III. DESIGN PROCEDURE

There are two basic approaches to implement distributed maximum power tracking into a PV system: module integrated DC-DC converters and module integrated DC-AC converters (inverters). In the DC approach, considered in this paper, converters are connected to the central inverter over the common DC bus. Again, there are two categories: parallel approach with all module integrated converters connected in parallel and series approach with parallel connected strings of DC-DC converters. Former approach is more flexible but requires high step-up conversion to meet the input voltage requirements for the central inverter. This can result in increased number of magnetic components and impaired efficiency. Later approach, considered in this paper, uses simpler topologies, but, due to the lower gain, requires multiple converters connected in strings to achieve high voltage of the DC bus and multiple strings connected in parallel to reach the desired power level (Fig. 4a). In the following analysis, interleaved boost converter will be designed to compare the performance of Si and GaN based devices. The basic converter circuit diagram is illustrated in Fig. 4b. The boost converter has proven as a simple and robust topology. By using interleaving, component stresses can be reduced and, at the same time, losses can be spread over the larger area, helping the thermal management. Since the main goal is to compare the switching performances, the converters were made using standard cores for inductors and only the losses in active components were considered.

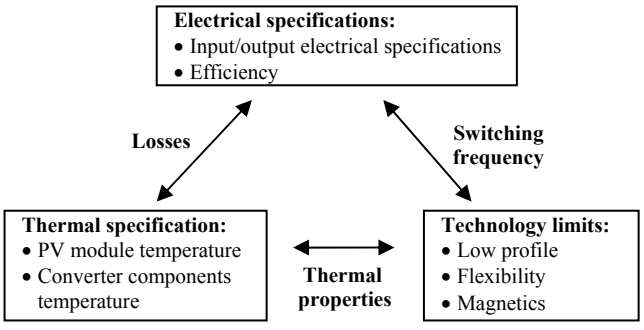

Figure 3. Interdependence between the design areas of the integrated covnerter

A. *Design goals and boundary conditions*

According to Fig. 3, the design process is determined by three sets of design specifications. Some of the specifications are already set; for example, the converter power level and input voltage/current ratings are determined by the PV module. Other specifications, like switching frequency or allowed losses, can be varied to make trade-offs between the design goals. In the considered converter, the main design specifications are listed as follows:

1) Electrical design: As already mentioned, the converter ratings are predetermined by the used PV module; in this case, the available module has a maximum power point voltage in the range from 8V to 17V, for the power range from 5W to 117W. For the sake of simplicity, the design procedure will be carried out for fixed input and output voltages. The input voltage is set to 15V, which corresponds to the maximum power point voltage for standard test conditions. The nominal output voltage is considered to be 48V. The switching frequency, being the design parameter, is used to make a trade-off in the design between efficiency/losses and the size of passive components. For the chosen switching frequency, the inductance value is calculated under condition that 30% current ripple is obtained. Afterwards, the values of input and output filter capacitors are calculated to achieve required voltage ripple; in this case, 0.5% at the input and 1% at the output side. With all circuit parameters known, the next step is to estimate power losses. For the following analysis only the power losses in the active components are considered

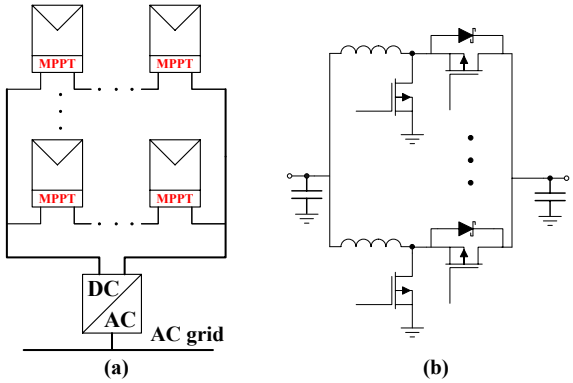

Figure 4. (a) System architecture, (b) Converter topology

since these components represent system parts with highest power loss density and the major contributors to the maximum reached temperatures. The loss calculation for the active devices is based on piecewise-linear approximation of device's terminal currents and voltages [13]. The resulting power losses serve as input data for the thermal analysis.

2) Thermal design: Because the converter will operate at high temperatures, it is important to estimate the temperature profile of the system, with special attention paid on the hot-spot location on the PV module where the converter is integrated, since this is the place with the highest power loss density. This is achieved by using a thermal model which takes the heat losses (from the electrical design) and loss distribution (spatial design and thermal management) as input variables and gives, as the result, the prediction of the system temperature behavior [14]. It can be shown that, with a good thermal management and efficient heat spreading, the temperature of the components of the integrated converter, on one side, and that of the PV module hot-spot, on the other side, will reach similar levels. The fact that the maximum operating temperature of the PV module (in the range of 90°C-100°C) is much lower than that of the converter components (usually 125°C or more), means that the PV module hot-spot temperature sets the critical design limit. Therefore, the maximum hot-spot temperature T_{crit} will set the upper limit for the switching frequency. In the following analysis T_{crit} was considered to be 90°C and, as a result of the thermal model, the amount of losses in active devices that leads to this temperature is approximately 3.5W.

3) Technology: The main technology design goals, with respect to the technology used for the PV module integrated converter, are very low profile and flexible construction. The major obstacle to achieve these goals is the boost inductor, in the first place the core material. While it is possible to use polymer-like laminates filled with ferrite powder, their permeability is very low (μ_r~10) [15], which limits the inductance values that can be achieved. On the other hand, large inductance is needed in order to decrease the current ripple and associated core losses, since the aforementioned materials are rather lossy. However the upper limit for the inductance value is determined by volumetric constraints. Large inductance results in higher number of turns which, considering the minimum wire cross-section area determined by inductor current capacity and conduction losses, increases the size of the inductor. This introduces the additional design limit parameter, the maximum allowed inductance value L_{crit}. For the following analysis, L_{crit} was set to 10μH.

Considering the filter capacitors, their values are determined by maximum allowed voltage ripple. In general, the relation between the voltage ripple Δv, inductance L, capacitance C and switching frequency f_{sw} is given with:

$$LC\Delta v = \frac{K}{f_{SW}^2}, \qquad (1)$$

where K is the constant that depends on converter circuit and operation mode. Later on it will be shown that, for the considered range of L and required voltage ripple, values of input and output capacitors are not critical, and can be easily achieved on a small surface area by paralleling low profile ceramic chip capacitors.

B. Design procedure

The design process flowchart is shown in Fig. 5. The design process is conducted for the full output power, since this scenario corresponds to the worst case condition with maximum power losses and reached temperatures. The design starts with predefined parameters - the converter voltage/current ratings and power level set by the PV module and system architecture, and initial variable parameters - switching frequency f_{sw} and number of phases N_{ph}. In the next step, the inductance value is obtained in order to achieve predetermined inductor current ripple. If the inductance results in high values, for the given switching frequency the number of phases has to be increased. With the determined inductor value the next step is to obtain the values of the filter capacitors, according to the required voltage ripple. Afterwards, the losses are calculated and used as inputs to the thermal model. The maximum hot-spot temperature is obtained from the thermal analysis and compared to the maximum allowed temperature to check if the design has to be redone with a modified switching frequency. This iterative process is repeated until the optimal values for the switching frequency and the inductor are obtained.

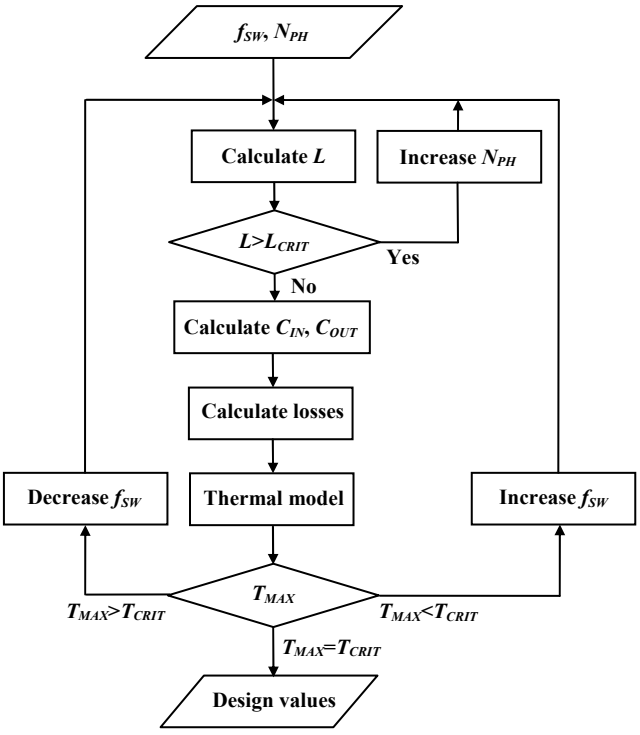

Figure 5. Design procedure for the PV module integrated converter

C. Device selection

To obtain the most optimal performance, the design procedure was performed for a range of available GaN and Si devices. According to the loss analysis, the main contributors to the losses are the device gate charge Q_g, on-resistance R_{on} and output capacitance C_{oss}. It is interesting to see the relation between considered devices in terms of figures of merit. This is illustrated in Fig. 6, where the comparison between the considered 100V devices is based on two figures of merit, $Q_g \cdot R_{on}$ and $C_{oss} \cdot R_{on}$. It should be noted that low figures of merit do not necessarily guaranty the lowest possible losses, since the gate drive circuit and the mode of operation can have significant influence on the final efficiency.

For the GaN based converter two devices were considered – EPC2001 and EPC 1007 [16]. The performed analysis shows that, despite having increased on-resistance, the later device can allow lower losses at higher operating frequencies due to the lower Q_g and C_{oss}. The former device is more suitable for lower operating frequencies and higher power levels. For this design, the boundary between aforementioned devices is in the vicinity of 400kHz. The final design was, due to the practical limitations of hand soldering, based on EPC2001. Concerning the Si based converter, the most suitable device was found to be IPI26CN10 (Infineon). However it should be noted that, due to the available packaging (TO-263), this device is not suitable for very low profile designs.

The main results of the design process for both GaN and Si device are presented in Table I. As expected, the higher operating frequency of the GaN based converter results in the two times smaller values of the boost inductor and filter capacitors, which can significantly reduce the size and cost of the converter. Also, the minimum required capacitances for both versions of the converter can be easily achieved by paralleling small low-profile ceramic capacitors, making the filter capacitors not so critical components as the boost inductor.

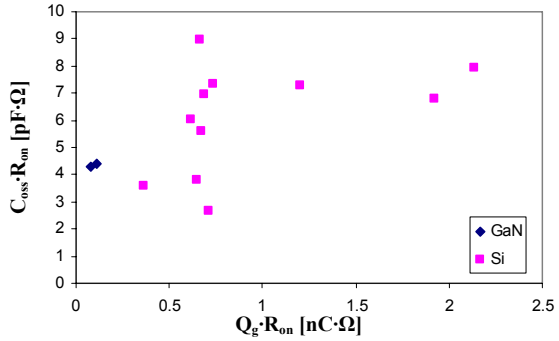

Figure 6. Figures of merit for 100V GaN and Si devices

TABLE I. CONVERTER SPECIFICATIONS

Parameter	f_{sw} [Hz]	N_{PH}	L [µH]	C_{in} [µF]	C_{out} [µF]	$P_{loss,act}$ [W]
Si converter	300	2	8.3	2.8	5.7	3.44
GaN converter	600	2	4.2	1.5	3	3.29

IV. EXPERIMENTAL AND MEASUREMENT RESULTS

To validate the results of the previous analysis, two prototype converters, shown in Fig. 7a, were built according to the specifications from Table I. The 8.3µH inductor for the Si based converter was made using E/PLT22 core (3F3 material) with four turns of litz wire. On the other side, the smaller 4.2µH inductance for the GaN based converter was made using smaller E/PLT18 core (3F3 material) and also using four turns of litz wire. The same gate drivers were used for both versions of the converter (EL7158). The switching waveforms for the GaN based converter under full load conditions (117W) are shown in Fig. 7b.

To obtain the losses in active components, first the overall efficiency of the converter was measured, not including the gate drive circuit consumption. After that, the inductor losses were obtained using the calorimetric measurements. Subtracting the inductor losses from total losses results in power losses in active devices, with assumption of small power losses in input and output capacitors. Table II shows the loss breakdown and measured efficiency for both versions of the converter operating at full power level. Comparing the results from Table I and II, it can be seen that the loss analysis underestimates the losses in active devices. As already mentioned, the loss estimation in the design process is based on the piecewise linear model where device capacitances completely determine its switching behavior. However, in practice when using

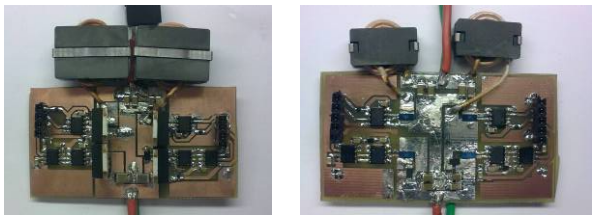

(a)

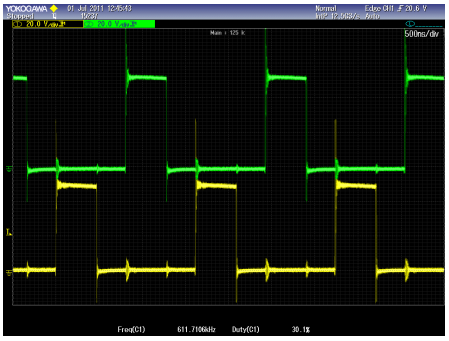

(b)

Figure 7. (a) Built converter prototypes, (b) Switching vaweforms (GaN converter)

TABLE II. BREAKDOWN OF CONVERTER LOSSES

Parameter	$P_{loss,total}$ [W]	$P_{loss,ind}$ [W]	$P_{loss,act}$ [W]	η [%]
Si converter	6.2	0.96	5.24	94.7
GaN converter	4.9	1.1	3.8	95.9

high-speed devices, parasitic inductances of the device leads and the PCB layout limit the switching process. This calls for improved analytical loss models for power devices that includes all relevant parasitic elements [17], and this will be considered in future work when designing the final version of the integrated converter.

Fig. 8 compares the conversion efficiencies as a functions of input power. According to the efficiency curves, both converters perform similar in terms of power losses and maximum reached efficiency. However, for the same performance, higher operating frequency of the GaN based converter allows for smaller passives and increased power density.

It is also interesting to see the performance of the GaN based converter when the switching frequency is further increased. Fig. 9 shows the efficiency curve for the operation under maximum power level, for switching frequencies increased up to 1MHz. As expected, the efficiency is reduced, although the high frequency performance can be improved using better cores, for example based on 3F4 material which is more suitable for higher switching frequencies. Therefore further reduction in size of passive components is possible if higher power losses are allowed.

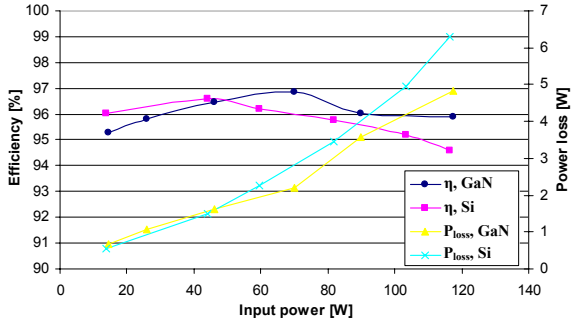

Figure 8. Measured conversion efficiencies and total power losses as a function of input power

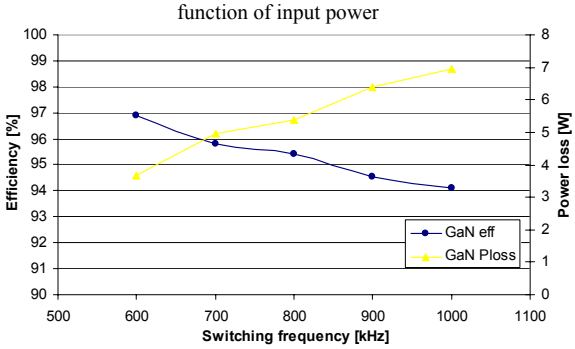

Figure 9. Measured conversion efficency as a function of switching frequency for the GaN converter

V. CONCLUSION

With its superior switching characteristics, the widespread use of GaN devices in power electronic applications is a near reality. Improved switching behavior will lead toward more efficient power conversion and, at the same time, will allow higher switching frequencies and lower cost through the reduction in size of passive components. This is especially beneficial for PV applications where cost effectiveness and high efficiency represent the most important requirements. This paper presents a performance comparison of commercially available GaN and Si devices through the design process of a PV module integrated converter. The presented analysis shows that GaN based converter is capable of operating at two times higher switching frequency while achieving the same performances as the Si based converter. This allows for substantial reduction in size of passive components and leads toward effective integration of the power electronic converter into the PV module.

REFERENCES

[1] E. Waffenschmidt, B. Ackermann, J.A. Ferreira, "Design Method and Material Technologies for Passives in Printed Circuit Board Embedded Circuits," IEEE Transactions on Power Electronics, Vol. 20, p. 576, May 2005

[2] I. Josifovic, J. Popovic-Gerber, J.A. Ferreira, "A PCB System Integration Concept for Power Electronics," Power Electronics and Motion Control Conference, IPEMC, May 2009

[3] S.L. Colino, R.A. Beach, "Fundamentals of Gallium Nitride Power Transistors," www.epc-co.com

[4] W.Yifeng, M.Jacob-Mitos, M.L.Moore, S.Heikman, "A97.8% efficient GaN HEMT boost converter with 300-W output power at 1MHz," IEEE Electron Device Letters, Vol. 29, p. 824, August 2008

[5] W.Saito, T.Nitta, Y.Kakiuchi, Y.Saito, K.Tsuda, I.Omura, M.Yamaguchi, "A 120-W Boost Converter Operation Using a High-Voltage GaN-HEMT," IEEE Electron Device Letters, Vol. 29, p. 8, January 2008

[6] J. Everts, J. Das, J. Van den Keybus, J. Genoe, M. Germain, J. Driesen, "A high-efficiency, high-frequency boost converter using enhancement mode GaN DHFETs on silicon," Energy Conversion Congress and Exposition (ECCE), November 2010

[7] D. Costinett, H. Nguyen, R. Zane, D. Maksimovic, "GaN-FET based dual active bridge DC-DC converter," Applied Power Electronics Conference and Exposition (APEC), April 2011

[8] N. Femia, G. Lisi, G. Petrone, G. Spagnuolo, M. Vitelli, "Distributed Maximum Power Point Tracking of Photovoltaic Arrays: Novel Approach and System Analys," IEEE Transactions on Industrial Electronics, Vol. 55, p. 2610, July 2008

[9] E.A.G. Hamers, M.N. van den Donker, B. Stannowski, R. Schlatmann, G.J. Jongerden: "Helianthos: Roll-to-Roll Deposition of Flexible Solar Cell Modules," Plasma Processes and Polymers, Vol. 4, p. 275, 2007

[10] J. Popovic, J. A. Ferreira, "An Approach to Deal with Packaging in Power Electronics," IEEE Transactions on Power Electronics, Vol. 20, No. 3, May 2005

[11] T. Nordmann, L. Clavadetscher, "Understanding Temperature Effects on PV System Performance," 3rd world conference on photovoltaic energy conversion, May 2003

[12] E. Waffenschmidt, B. Ackermann, M. Wille, "Integrated Ultra Thin Flexible Inductors for Low Power Converters," Power Electronics Specialists Conference, June 2005

[13] Klein, J, "Synchronous Buck Mosfet Loss Calculation with EXEL Model," Fairchild Semiconductor Application note AN-6005

[14] M. Acanski, J. Popovic-Gerber, J.A. Ferreira, "Thermal Modeling of the Module Integrated DC-DC Converter for Thin-Film PV Modules," Power Electronics and Motion Control Conference, EPE-PEMC2010, September 2010

[15] EPCOS, "Ferrite Polymer Composite (FPC) Film," http://www.epcos.com/inf/80/ap/e0001000.htm

[16] www.epc-co.com

[17] M. Rodriguez, A. Rodriguez, P.F. Miaja, D.G. Lamar, J.S. Zuniga, "An Insight into the Switching Process of Power MOSFETs: An Improved Analytical Losses Model," IEEE Transactions on Power Electronics, Vol. 25, p.1626, June 2010